

Modelling Spatial Interactions in the Arbuscular Mycorrhizal Symbiosis using the Calculus of Wrapped Compartments*

Cristina Calcagno¹, Mario Coppo², Ferruccio Damiani², Maurizio Drocco²
Eva Sciacca², Salvatore Spinella² and Angelo Troina²

¹Dipartimento di Biologia Vegetale, Università di Torino

²Dipartimento di Informatica, Università di Torino

Arbuscular mycorrhiza (AM) is the most wide-spread plant-fungus symbiosis on earth. Investigating this kind of symbiosis is considered one of the most promising ways to develop methods to nurture plants in more natural manners, avoiding the complex chemical productions used nowadays to produce artificial fertilizers. In previous work we used the Calculus of Wrapped Compartments (CWC) to investigate different phases of the AM symbiosis. In this paper, we continue this line of research by modelling the colonisation of the plant root cells by the fungal hyphae spreading in the soil. This study requires the description of some spatial interaction. Although CWC has no explicit feature modelling a spatial geometry, the compartment labelling feature can be effectively exploited to define a discrete surface topology outlining the relevant sectors which determine the spatial properties of the system under consideration. Different situations and interesting spatial properties can be modelled and analysed in such a lightweight framework (which has not an explicit notion of geometry with coordinates and spatial metrics), thus exploiting the existing CWC simulation tool.

1 Introduction

Arbuscular mycorrhiza (AM) is the most wide-spread plant-fungus symbiosis on earth [25]. Investigating this kind of symbiosis is considered one of the most promising ways to develop methods to nurture plants in more natural manners, avoiding the complex chemical productions used nowadays to produce artificial fertilizers.

In previous works [17, 45] in the context of the BioBITS project [11] we investigated different phases of the AM symbiosis by using the Calculus of Wrapped Compartments (CWC) [19], a variant of the Calculus of Looping Sequences (CLS) [7, 6]. These calculi have been designed to represent in a formal way biological entities such as molecules, DNA strands and cells. Starting from an alphabet of atomic elements (*atoms* for short) and from an alphabet of *labels*, CWC terms are defined as multisets of atoms and compartments. A compartment consists of a *wrap* (a multiset of atoms detailing the elements of interest on the membrane), a *content* (a term) and a *type* (a label). The evolution of the system is driven by a set of rewrite rules modelling the reactions of interest (elements interaction and movement). In previous work, we have introduced in CWC rules a notion of rate which allow CWC to be equipped with a semantics given in terms of Continuous Time Markov Chains (CTMCs), thus enabling stochastic simulation built following the standard Gillespie's approach [24]. Moreover, we have defined a hybrid simulation algorithm to speed up the simulation procedure while keeping the exactness of Gillespie's method, [18]. The simulation tool [2] has been integrated in the FastFlow [4] programming framework for the execution of parallel simulations in multi-core platforms [3].

*This research is funded by the BioBITS Project (*Converging Technologies* 2007, area: Biotechnology-ICT), Regione Piemonte.

In this paper, we continue our ongoing research on the AM symbiosis by modelling the colonization of the plant root cells by the fungal hyphae spreading in the soil. The interaction begins with a molecular dialogue between the plant and the fungus. Host roots release signalling molecules characterized as strigolactones which induce alterations in the fungal physiology and hyphal branching. In response to the plant signal AM fungi produce a symbiotic signal, the “Myc Factor”. One of the first response observed in epidermal plant root cells is a repeated oscillation of Ca^{2+} concentration preparing to the reorganization of the cell for the fungal penetration. Following this event, fungal hyphae enter and cross the epidermal cells, growing inter- and intracellularly all along the root in order to spread fungal structures. Once inside the inner layers of the cortical cells, specialised fungal hyphae differentiate into arbuscules where the nutrients exchange between the two organisms occur.

To represent this kind of behaviour we need to model some spatial properties of the system like the movement of the hyphae in the soil and their penetration and articulation in the root tissue. To this aim we exploit the fact that the notion of compartment can also be used, in a very natural way, to represent spatial regions (with a fixed topology) in which the labels play a key role in defining the spatial properties. These kind of compartments are thus considered as the topological sectors in the analysed model. In this framework, the movement and growth of system elements are described via specific rules (involving adjacent compartments) and the functionalities of biological components can be affected by the spatial constraints given by the sector in which they interact with other elements. A similar approach can be found in [34] where the topological structure of the components is expressed via explicit links which require ad-hoc rules to represent movements of biological entities.

Although our approach does not support an explicit representation of continuous space, we can exploit the topological structure of compartments, their inter-relations, and their relative placement as a starting point to implicitly define spatial properties. This level of abstraction is suitable to model some situations where it is not needed to explicitly specify the space occupied by the elements of the system. Avoiding to introduce explicit features for modeling a spatial geometry (e.g., coordinates, position, extension, motion direction and speed, rotation, collision and overlap detection, communication range, etc.) may in some cases reduce the complexity of the models and simplify the analysis of the system and the simulation procedure.

1.1 Summary

The remainder of the paper is organised as follows. In Section 2 we recall the syntax and semantics of CWC. In Section 3, through a few chosen paradigmatic examples, we start giving some hint about spatial modelling and analysis within the CWC framework. In Section 4 we exploit the approach to model some spatial interaction in the Arbuscular Mycorrhizal Symbiosis. In particular, we show how molecules (carrying the communication signals between the plant and the fungus) diffuse in the soil, and how the fungus contacts, through its hyphae, the cells of the plant root. Finally, in Section 5 we briefly discuss related and possible future work and draw our conclusions.

2 The Calculus of Wrapped Compartments

The Calculus of Wrapped Compartments (CWC) (see [19, 17]) is based on a nested structure of ambients delimited by membranes with specific properties. Biological entities like cells, bacteria and their interactions can be easily described in CWC.

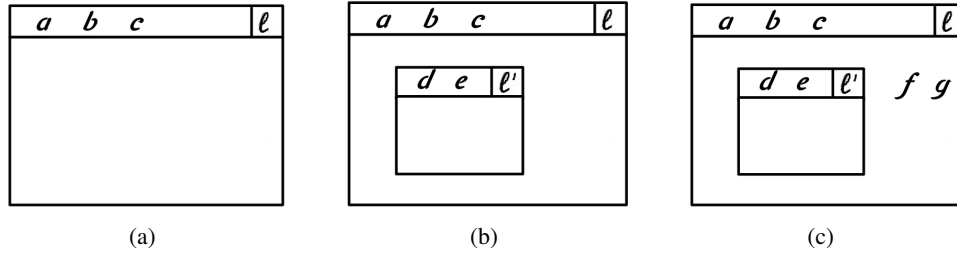


Figure 1: **(a)** represents $(a \ b \ c \mid \bullet)^\ell$; **(b)** represents $(a \ b \ c \mid (d \ e \mid \bullet)^{\ell'})^\ell$; **(c)** represents $(a \ b \ c \mid (d \ e \mid \bullet)^{\ell'} \ f \ g)^\ell$

2.1 Syntax

Let \mathcal{A} be a set of *atomic elements* (*atoms* for short), ranged over by a, b, \dots , and \mathcal{L} a set of *compartment types* represented as *labels* ranged over by ℓ, \dots . A *term* of CWC is a multiset \bar{t} of *simple terms* where a simple term is either an atom a or a compartment $(\bar{a} \mid \bar{t}')^\ell$ consisting of a *wrap* (represented by a multiset of atoms \bar{a})¹, represented by a (possibly empty) and a *content*, represented by a term \bar{t}' and a *type*, represented by the label ℓ . An empty multiset is represented symbolically with “ \bullet ”.

As usual, the notation $n * t$ denotes n occurrences of the simple term t . An example of term is $2 * a \ b \ (c \ d \mid e \ f)^\ell$ representing a multiset (multisets are denoted by listing the elements separated by a space) consisting of two occurrences of a , one occurrence of b (e.g. three molecules) and an ℓ -type compartment $(c \ d \mid e \ f)^\ell$ which, in turn, consists of a wrap (a membrane) with two atoms c and d (e.g. two proteins) on its surface, and containing the atoms e (e.g. a molecule) and f (e.g. a DNA strand). See Figure 1 for some other examples with a simple graphical representation.

2.2 Rewriting Rules

System transformations are defined by rewriting rules written over an extended set of terms including variables. The l.h.s. component of a rewrite rule \bar{p} is called *pattern* and the r.h.s. component \bar{o} of a rewrite rule is called *open term*. Patterns and open terms are multiset of *simple patterns* p and *simple open terms* o defined by the following syntax:

$$\begin{array}{ll} p & ::= a \mid (\bar{a} \mid x \mid \bar{p} \ X)^\ell \\ o & ::= a \mid (\bar{a} \mid x \mid \bar{o})^\ell \mid X \end{array}$$

where \bar{a} is a multiset of atoms, x and X are variables that can be instantiated, respectively by a multiset of atoms (on a wrap) or by a term (in the compartment contents). The label ℓ is called the *type of the pattern*. Patterns are intended to match, via substitution of variables, with simple terms and compartments occurring as subterms of the term representing the whole system. Note that we force *exactly* one variable to occur in each compartment content and wrap. This prevents ambiguities in the instantiations needed to match a given compartment.²

A *rewrite rule* is a triple (ℓ, \bar{p}, \bar{o}) , denoted by $\ell : \bar{p} \mapsto \bar{o}$, where \bar{p} and \bar{o} are such that the variables occurring in \bar{o} are a subset of the variables occurring in \bar{p} . The application of a rule $\ell : \bar{p} \mapsto \bar{o}$ to a term

¹the wrap of a compartment contains the elements characterizing the membrane enclosing it. So we assume that it cannot contain other compartments but only atomic elements (for instance proteins).

²The linearity condition, in biological terms, corresponds to the exclusion of transformations depending on the presence of two (or more) identical (and generic) components in different compartments (see also [39]).

\bar{t} is performed in the following way: 1) Find in \bar{t} (if it exists) a compartment of type ℓ with content \bar{u} and a substitution σ of variables by ground terms (i.e. terms without occurrences of variables) such that $\bar{u} = \sigma(\bar{p} X)$, where X is a variable not occurring in \bar{p} , \bar{o} ; and 2) Replace in \bar{t} the subterm u with $\sigma(\bar{o} X)$. We write $\bar{t} \mapsto \bar{t}'$ if \bar{t}' is obtained by applying a rewrite rule to \bar{t} .

For instance, the rewrite rule $\ell : a b \mapsto c$ means that in all compartments of type ℓ containing an occurrence of $a b$, it can be replaced by c . While the rewrite rule $\ell : (x \mid a b X)^{\ell_1} \mapsto (x \mid c X)^{\ell_2}$ means that, if contained in a compartment of type ℓ , all compartments of type ℓ_1 and containing an $a b$ in their content can change their type to ℓ_2 and an occurrence of $a b$ can be replaced by c .

Remark. For uniformity we assume that the term representing the whole system is always a single compartment labelled \top with an empty wrap, i.e., all systems are represented by a term of the shape $(\bullet \mid \bar{t})^\top$, which we will also write as \bar{t} for simplicity.

2.3 Stochastic Simulation

A stochastic simulation model for biological systems can be defined along the lines of the one presented by Gillespie in [24], which is, *de facto*, the standard way to model quantitative aspects of biological systems. The basic idea of Gillespie's algorithm is that a rate function is associated with each considered chemical reaction which is used as the parameter of an exponential distribution modelling the probability that the reaction takes place. In the standard approach this reaction rate is obtained by multiplying the kinetic constant of the reaction by the number of possible combinations of reactants that may occur in the region in which the reaction takes place, thus modelling the law of mass action. In [19], the reaction rate is defined in a more general way by associating to each reduction rule a function which can also define rates based on different principles as, for instance, the Michaelis-Menten nonlinear kinetics.

In the examples of this paper it is reasonable to assume a linear dependence of the reaction rate on the number of possible combinations of interacting components, so we will follow the standard approach in defining reaction rates. Each reduction rule is then enriched by the kinetic constant k of the reaction that it represents (notation $\ell : p \xrightarrow{k} o$). For instance in evaluating the application rate of the stochastic rewrite rule $R = \ell : a b X \xrightarrow{k} c X$ to the term $\bar{t} = a a b b$ in a compartment of type ℓ we must consider the number of the possible combinations of reactants of the form $a b$ in \bar{t} . Since each occurrence of a can react with each occurrence of b , this number is 4. So the application rate of R is $k \cdot 4$.

2.4 The CWC simulator

The CWC simulator [2] is a tool under development at the Computer science Department of Turin University, based on Gillespie's direct method algorithm [24]. It treats CWC models with different rating semantics (law of mass action, Michaelis-Menten kinetics, Hill equation) and it can run independent stochastic simulations over CWC models, featuring deep parallel optimizations for multi-core platforms on the top of FastFlow [4]. It also performs online analysis by a modular statistical framework.

3 Topological Interpretations within CWC

In this section we provide some hint about spatial modelling and analysis within the CWC framework by means of some paradigmatic examples. For simplicity, we will consider the compartments in our system to be *well-stirred*. Thus, also the compartments representing the spatial sectors of our topology will consist of well-mixed components. Note that the topological analysis described in the following

examples could be expressed also with other calculi with compartmentalisation such as, for example, BioAmbients [42], Brane Calculi [14] and Beta-Binders [21].

3.1 Cell Growth and Proliferation: A CWC Grid

Eukaryotic cells reproduce themselves by cell cycle which can be divided in two brief periods: the interphase during which the cell grows, accumulating nutrients and duplicating its DNA and the mitosis (M) phase, during which the cell splits itself into two distinct cells, often called “daughter cells”. Interphase proceeds in three stages, $G1$, S , and $G2$. $G1$ (Gap1) is also called the growth phase, and is marked by synthesis of various enzymes that are required in S phase, mainly those needed for DNA replication. In S phase (Synthesis) DNA replication occurs. The cell then enters the $G2$ (Gap2) phase, which lasts until the cell enters mitosis. Again, significant biosynthesis occurs during this phase, mainly involving the production of microtubules, which are required during the process of mitosis.

Spatial representation of the growth of cell populations could be useful in many situations (in the study of bacteria colonies, in developmental biology, and in the analysis of cancer cells proliferation).

Intuitively, we may express cell proliferation by describing a finite space through a CWC grid such that on each *grid cell* we can insert a cell of the growing population under analysis. An $k \times n$ grid could be modelled in CWC with $k * n$ compartment labels modelling the *grid cells*. A cell may grow in one of the adjacent *grid cells* (with a given scheme of adjacency modelled by the set of rewrite rules).

Intuitively, using the atomic element e to denote an empty *grid cell*, an empty grid could be modelled by the following CWC term:

$$\begin{aligned} \text{Prol_Grid} = & (\] e)^{1,1} \ \dots (\] e)^{1,n} \\ & (\] e)^{2,1} \ \dots (\] e)^{2,n} \\ & \dots \\ & (\] e)^{m,1} \ \dots (\] e)^{m,n} \end{aligned}$$

If we represent a cell of our population as a compartment with membrane m and with a single atom in its content representing the phase of the cell cycle (M , $G1$, S , $G2$), a *grid cell* i, j may contain the cell $(m \] M)^{cell}$ that could grow, with kinetic k_{mit} , towards the empty *grid cell* $i, j + 1$ with the rewrite rule ³:

$$\top \quad : \quad (x \] (m \ y \] M \ Y)^{cell} \ X)^{i,j} (z \] e \ Z)^{i,j+1} \xrightarrow{k_{mit}} (x \] (m \ y \] G1 \ Y)^{cell} \ X)^{i,j} (z \] (m \] G1)^{cell} \ Z)^{i,j+1}$$

while cells may change their internal state (cell cycle phase) with the rules:

$$\begin{aligned} i, j \quad : \quad (m \ x \] G1 \ X)^{cell} & \xrightarrow{k_{phase1}} (m \ x \] S \ X)^{cell} \\ i, j \quad : \quad (m \ x \] S \ X)^{cell} & \xrightarrow{k_{phase2}} (m \ x \] G2 \ X)^{cell} \\ i, j \quad : \quad (m \ x \] G2 \ X)^{cell} & \xrightarrow{k_{phase3}} (m \ x \] M \ X)^{cell} \end{aligned}$$

Note that each element of the grid can be occupied only by one cell, so this model allows only a limited growth of the cells, corresponding to the dimension of the grid. However this could be enough to investigate the properties of the cell growth.

³note that under our assumptions the variables will always match only with the empty multiset

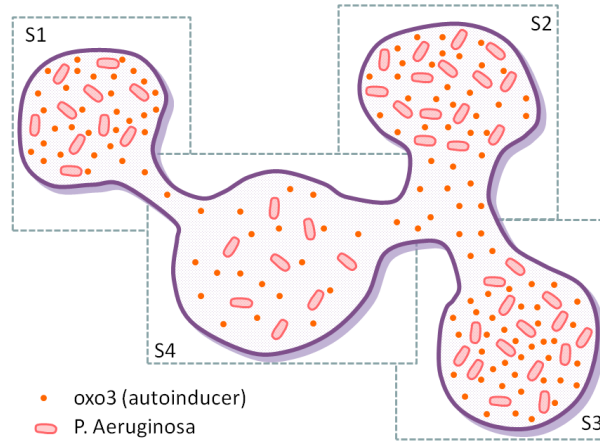


Figure 2: Quorum Sensing in a distributed topology.

3.2 Quorum Sensing and Molecular Diffusion

Molecular diffusion (or simply diffusion) arises from the motion of particles as a function of temperature, viscosity of the medium and the size (or mass) of the particles. Usually, diffusion explains the flux of molecules from a region of higher concentration to one of lower concentration, but it may also occur when there is no concentration gradient. The result of the diffusion process is a gradual mixing of the involved particles. In the case of uniform diffusion (given a uniform temperature and absent external forces acting on the particles) the process will eventually result in a complete mixing. Equilibrium is reached when the concentrations of the diffusing molecules between two compartments becomes equal.

Diffusion is of fundamental importance in many disciplines of physics, chemistry, and biology. In this subsection we will consider the diffusion of the auto-inducer communication signals in a quorum sensing process where the bacteria initiating the process are distributed in different sectors of an environment (see Figure 2). We consider the sectors of the environment to be connected through channels with different capacities and different speeds regulating the movement of the auto-inducer molecules between the different sectors.

The CWC model describing the system can be found in Appendix A. We modelled the four sectors as four different compartments with special labels S_i allowing the flow of the *oxo3* auto-inducer molecules with different speed. Bacteria (modelled as compartments with label m) were marked as “active” when they reached a sufficient high level of the *oxo3* auto-inducer. The results of a simulation running for 30 seconds is shown in Figure 3.

Although CWC does not have a direct mechanism to formulate the spatial position of its terms and a metric distance between them, it has the potential to describe topologically different spatial concepts. For example, the compartments are able, through the containment specification, to express discrete distance among the entities that are inside and those on the outside. Moreover, through the rule kinetics we are able to model space anisotropy (lack of uniformity in all orientations), which are useful to formulate complex concepts of reachability. The model discussed in this section is a clear example of these issues.

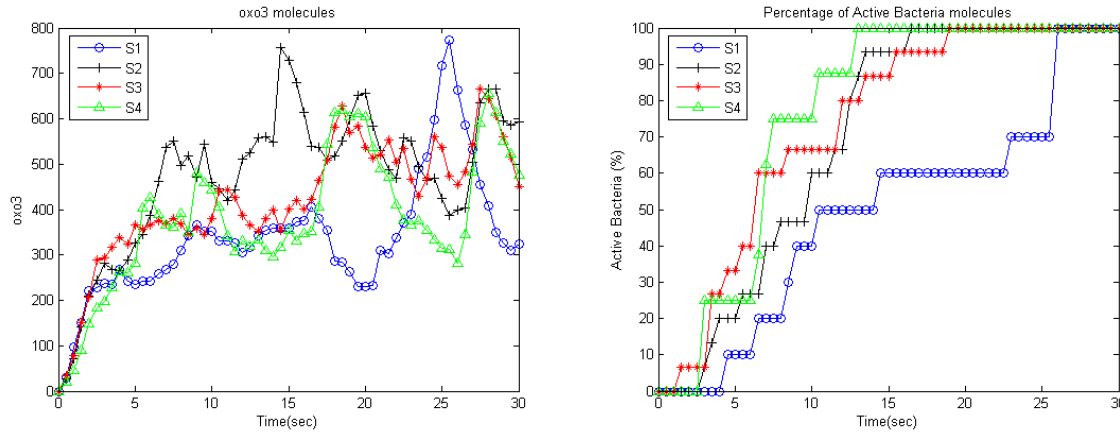


Figure 3: Simulation results of oxo3 molecules (left figure) and active bacteria percentage with respect to the total number of bacteria (right figure) in the different sectors.

4 Spatial Interactions in the Arbuscular Mycorrhizal Symbiosis

Arbuscular mycorrhizae, formed between 80% of land plants and arbuscular mycorrhizal (AM) fungi belonging to the Glomeromycota phylum, are the most common and widespread symbiosis on our planet [25]. AM fungi are obligate symbionts which supply the host with essential nutrients such as phosphate, nitrate and other minerals from the soil. In return, AM fungi receive carbohydrates derived from photosynthesis in the host. AM symbiosis also confers resistance to the plant against pathogens and environmental stresses. Despite the central importance of AM symbiosis in both agriculture and natural ecosystems, the mechanisms for the formation of a functional symbiosis between plants and AM fungi are largely unknown.

4.1 The Biological Interactions under Investigation

The interaction begins with a molecular dialogue between the plant and the fungus [25]. Host roots release signalling molecules characterized as strigolactones [1] which are sesquiterpenes derived from the carotenoid pathway [33, 32]. Within just a few hours, strigolactones at subnanomolar concentrations induce alterations in fungal physiology and mitochondrial activity and extensive hyphal branching [10]. Root exudates from plants grown under phosphate-limited conditions are more active than those from plants with sufficient phosphate nutrition, suggesting that the production of these active exudates in roots is regulated by phosphate availability [36, 47]. Strigolactones also appear to act as chemo-attractants: fungal hyphae of *Glomus mosseae* exhibited chemotropic growth towards roots at a distance of at least 910 μm in response to host-derived signals, possibly strigolactones [44]. Some solid evidence has been presented for AM fungal production of a long-hypothesized symbiotic signal, the “Myc Factor”, in response to the plant symbiotic signal. Fungal hyphae of the genus *Gigaspora* growing in the vicinity of host roots, but separated from the roots by a membrane, release a diffusible substance that induces the expression of a symbiosis-specific gene in *Medicago truncatula* roots [29]. This expression was correlated both spatially and temporally with the appearance of hyphal branching, and was not observed when hyphal branching was absent. The external signal released by these fungi is perceived by a receptor on the plant plasma membrane and is transduced into the cell with the activation of a symbiotic signalling

pathway that lead to the colonization process. One of the first response observed in epidermal cells of the root is a repeated oscillation of Ca^{2+} concentration in the nucleus and perinuclear cytoplasm through the alternate activity of Ca^{2+} channels and transporters [38, 30, 16]. Kosuta and colleagues [30] assessed mycorrhizal induced calcium changes in *Medicago truncatula* plants transformed with the calcium reporter cameleon. Calcium oscillations were observed in a number of cells in close proximity to plant/fungal contact points. Very recently Chabaud and colleagues [16] using root organ cultures of both *Medicago truncatula* and *Daucus carota* observed Ca^{2+} spiking in AM-responsive zone of the root treated with AM spore exudate.

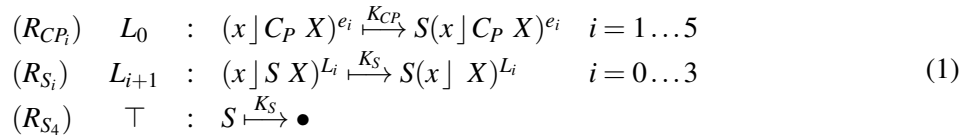
Once reached the root surface the AM fungus differentiates a hyphopodium via which it enters the root. A reorganization of the plant cell occurs before the fungal penetration: a thick cytoplasmic bridge (called pre-penetration apparatus -PPA-) is formed and it constitutes a trans-cellular tunnel in which the fungal hypha will grow [23]. Following this event, a hyphal peg is produced which enters and crosses the epidermal cell, avoiding a direct contact between fungal wall and host cytoplasm thanks to a surrounding membrane of host origin [22]. Then the fungus overcomes the epidermal layer and it grows inter-and intracellularly all along the root in order to spread fungal structures. Once inside the inner layers of the cortical cells the differentiation of specialized, highly branched intracellular hyphae called arbuscules occur. Arbuscules are considered the major site for nutrients exchange between the two organisms and they form by repeated dichotomous hyphal branching and grow until they fill the cortical cell. They are ephemeral structures [46, 27]: at some point after maturity, the arbuscules collapse, degenerate, and die and the plant cell regains its previous organization [12]. The mechanisms underlying arbuscule turnover are unknown but do not involve plant cell death. In arbuscule-containing cells the two partners come in intimate physical contact and adapt their metabolisms to allow reciprocal benefits.

4.2 The CWC Model

We model the Arbuscular Mycorrhizal symbiosis in a 2D space. The soil environment is partitioned into different concentric layers to account for the distance between the plant root cells and the fungal hyphae where the inner layer contains the plant root cells. The plant root tissue is also modelled as concentric layers each one composed by sectors.

For the sake of simplicity we modelled the soil into 5 different concentric layers (modelled as different compartments labelled by L_0 - L_4 identifying L_4 with the top level \top). Although the root has a complex layered structure we simplified it into 3 concentric layers (one epidermal layer and 2 cortical layers) each one composed by 5 sectors mapped as different compartments labelled by e_i ($i = 1 \dots 5$) for epidermal cells and c_{jk} ($j = 1, 2$ and $k = 1 \dots 5$) for cortical cells. Exploiting the flexibility of CWC, compartment labels are here used to characterize both their spatial position and their biological properties. All the compartments and the main atoms of the model are depicted in Figure 4.

The stigolactones (atoms S) derived from the carotenoid pathway (atom C_P) are released by epidermal cells and can diffuse through the soil degrading their activity when farthest from the plant. This situation was modelled by the following rules:



Since phosphate (atoms P) conditions regulate strigolactones biosynthesis inhibiting the carotenoid

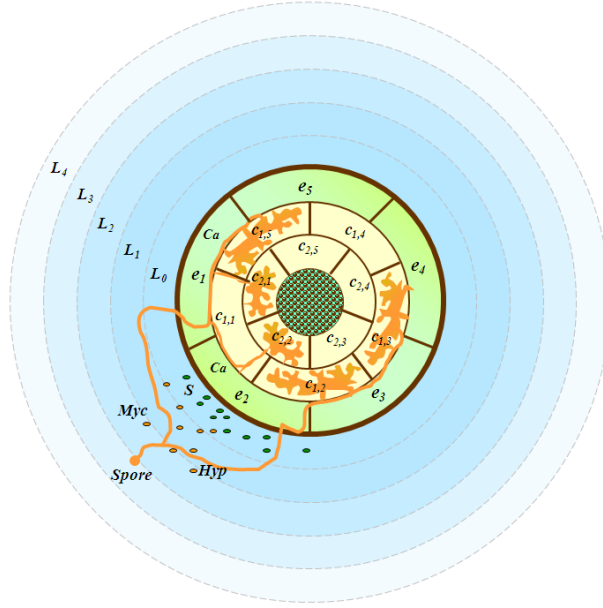


Figure 4: 2D spatial model of the Arbuscular Mycorrhizal symbiosis.

pathway (atom IC_P), the following rules were considered :

$$(R_{IC_P}) \quad L_0 : P(x \mid C_P X)^{e_i} \xrightarrow{K_{IC_P}} P(x \mid IC_P X)^{e_i} \quad i = 1 \dots 5 \quad (2)$$

The fungal structure is described by atoms where each atom represents a particular type of fungal component. The atom *Spore* represents the fungal spore while atoms *Hyp* represent fungal hyphae. AM fungal hyphae branching towards the plant root is regulated by the strigolactones activity. If we locate the fungal spore at a fixed distance from the plant root (let us say at the layer L_k where $0 < k < 4$) then the spore hyphal branching is generated stochastically in the relative inferior and superior layers. In our experiments the fungal spore was placed at the soil layer L_2 . The hyphal branching is radial with respect to the spore position causing a branching away from the spore and promoted at the proximity of the root by the strigolactones. This branching process was represented by the following rules:

$$\begin{aligned} (R_{F_1}) \quad L_2 &: Spore(x \mid X)^{L_1} \xrightarrow{K_F} Spore(x \mid Hyp X)^{L_1} \\ (R_{F_2}) \quad L_3 &: (x \mid Spore X)^{L_2} \xrightarrow{K_F} Hyp(x \mid Spore X)^{L_2} \\ (R_{H_j}) \quad \top &: (x \mid Hyp X)^{L_3} \xrightarrow{K_H} Hyp(x \mid Hyp X)^{L_3} \\ (R_{H_1}) \quad L_1 &: S Hyp(x \mid X)^{L_0} \xrightarrow{K_{H_1}} S Hyp(x \mid Hyp X)^{L_0} \end{aligned} \quad (3)$$

The AM fungal production of Myc factor (atom *Myc*) at the proximity of the root cells inducing the calcium spiking phenomenon (atom *Ca*) at a responsive state (atom *Resp*) which prepares the epidermal cells to include the fungal hyphae was modelled by the following rules:

$$\begin{aligned} (R_{Myc}) \quad L_0 &: Hyp \xrightarrow{K_M} Myc Hyp \\ (R_{MycCa_i}) \quad L_0 &: Myc(Resp x \mid X)^{e_i} \xrightarrow{K_{MC}} (Resp x \mid Ca X)^{e_i} \quad i = 1 \dots 5 \\ (R_{Ca_i}) \quad L_0 &: Hyp(Resp x \mid Ca X)^{e_i} \xrightarrow{K_{Ca}} Hyp(NResp x \mid Hyp X)^{e_i} \quad i = 1 \dots 5 \end{aligned} \quad (4)$$

where the epidermal cells change their state from responsive to not responsive (atom $NResp$) since they can be penetrated by only one hypha.

Once the fungal hyphae penetrate the epidermal cells they are allowed to branch in the two directions of the underneath cortical layer and from this cortical layer to the inner one. The cortical cells change their state from responsive (atom $Resp$) to transitive (atom $Trans$) and then to mycorrhized (atom Arb) since an hypha can grow in the cortical intercellular spaces even if already mycorrhized but only one arbuscule can be generated. The hyphal branching from the epidermal layer to the cortical layers is modelled through the following rules:

$$\begin{aligned}
 (R_{CB1i}) \quad L_0 &: (NResp \ x \rfloor Hyp \ X)^{e_i} (Resp \ y \rfloor Y)^{c_{1j}} \xrightarrow{K_{CB}} (NResp \ x \rfloor Hyp \ X)^{e_i} (Trans \ y \rfloor Hyp \ Y)^{c_{1j}} \\
 &\quad i = 1 \dots 5, j = i(mod5), i + 1(mod5); \\
 (R_{CB12i}) \quad L_0 &: (Trans \ x \rfloor Hyp \ X)^{c_{1i}} (Resp \ y \rfloor Y)^{c_{2j}} \xrightarrow{K_{CB}} (Trans \ x \rfloor Hyp \ X)^{c_{1i}} (Trans \ x \rfloor Hyp \ Y)^{c_{2j}} \\
 &\quad i = 1 \dots 5, j = i(mod5), i + 1(mod5); \\
 (R_{CB22i}) \quad L_0 &: (Arb \ x \rfloor Hyp \ X)^{c_{1i}} (Resp \ y \rfloor Y)^{c_{2j}} \xrightarrow{K_{CB}} (Arb \ x \rfloor Hyp \ X)^{c_{1i}} (Trans \ y \rfloor Hyp \ Y)^{c_{2j}} \\
 &\quad i = 1 \dots 5, j = i(mod5), i + 1(mod5);
 \end{aligned} \tag{5}$$

Finally, the modelling of each fungal hyphae penetrated into a cortical cell to create an arbuscule (atom A) and start the symbiosis is performed by the following rules:

$$(R_{Aij}) \quad L_0 : (Trans \ x \rfloor Hyp \ X)^{c_{ij}} \xrightarrow{K_A} (Arb \ x \rfloor Hyp \ X)^{c_{ij}} \quad i = 1, 2; j = 1 \dots 5 \tag{6}$$

4.3 Simulation Results

The initial term describing our system is given by T :

$$\begin{aligned}
 T = & \left(\rfloor \left(\rfloor \left(\rfloor Spore \left(\rfloor \left(\rfloor T' \right)^{L_0} \right)^{L_1} \right)^{L_2} \right)^{L_3} \right)^\top \\
 & \text{where} \\
 & T' = V \ U \\
 & V = V_1 \ V_2 \ V_3 \ V_4 \ V_5 \\
 & V_i = (Resp \rfloor C_P)^{e_i} \\
 & U = U_{11} \ U_{12} \ U_{13} \ U_{14} \ U_{15} \ U_{21} \ U_{22} \ U_{23} \ U_{24} \ U_{25} \\
 & U_{jk} = (Resp \rfloor)^{c_{jk}}
 \end{aligned} \tag{7}$$

The model has been used to virtually simulate 21 days of the fungus–plant interactions. The reaction rates have been chosen to resemble the experimental observations of “in vivo” fungal germination, hyphal branching and arbuscules creation under similar environmental conditions of the simulations. The rates were set as following: $K_{CP} = 0.8$, $K_S = 0.1$, $K_{ICP} = 0.01$, $K_F = 0.2$, $K_H = 0.05$, $K_{H_1} = 0.01$, $K_M = 0.2$, $K_{MC} = 0.2$, $K_{Ca} = 1.0$, $K_{CB} = 0.9$, $K_A = 1.0$. In Figure 5 we show a surface plot representing an exemplification of the CWC simulation about strigolactones diffusion (on the left) and fungal hyphal branching (on the right) along the soil layers during time.

We compared our simulation results adding the phosphate (100 P atoms) to the soil layers yielding to the results given by Figure 6. In this case we have a lower strigolactones production by the root cells and an hyphal branching not promoted in the direction of the root.

We performed 60 simulations in the three conditions of low phosphate (10 P atoms), medium phosphate (50 P atoms) and high phosphate (100 P atoms) conditions leading to a 60% of arbuscules in the

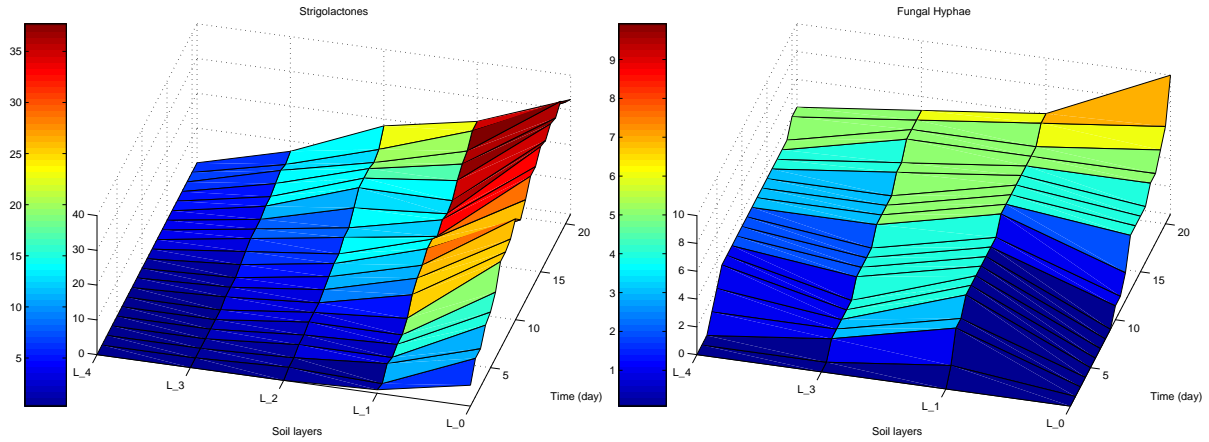


Figure 5: Simulation results of strigolactones diffusion (left figure) and fungal hyphal branching (right figure) along the soil layers during time.

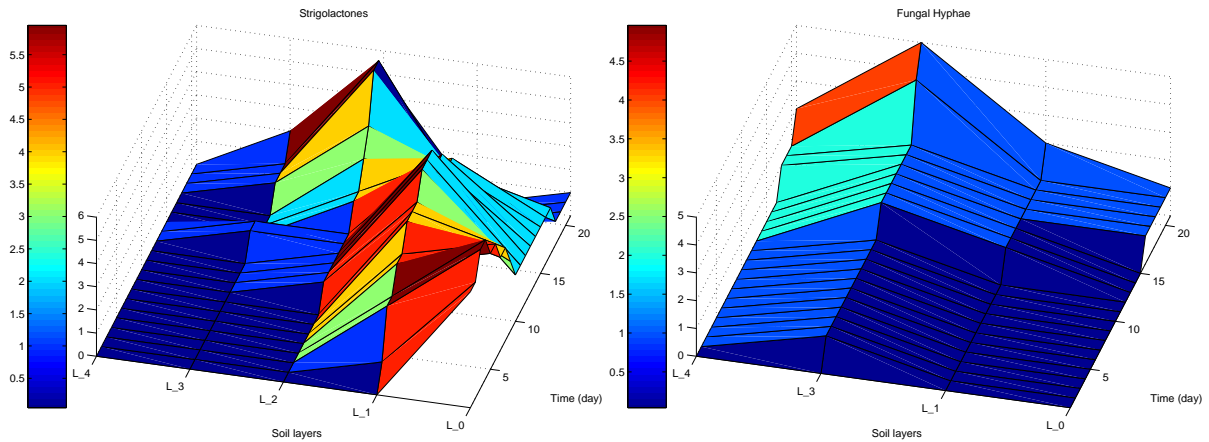


Figure 6: Simulation results of strigolactones diffusion (left figure) and fungal hyphal branching (right figure) along the soil layers at high phosphate concentrations.

first case, 30% in the second case, and 10% in the latter case. The first arbuscules occur around the 8th – 9th day of simulation at low phosphate condition while they are formed from the 9th to the 15th day at high phosphate conditions. These results reflect the in vivo experiments on several plants inoculated with different AM fungi [35, 5, 26].

Our long term goal is to design a virtual spatial model that would enable us to test “in silico” various hypotheses about the interaction between the physiological processes that drive the arbuscular mycorrhizal symbiosis and the signalling processes that take place in this symbiosis.

5 Conclusions, Related and Further Work

In the last few years, computer scientists have developed several languages and tools to build and analyse models of biological systems, often relating different behaviour that operates on different levels of abstraction and on different time and spatial scales [40, 41, 43, 20, 14, 21, 31].

This work constitutes a first step towards providing CWC with the features required by the emerging field of *spatial systems biology*, which aims at integrating the analysis of biological systems with spatial properties.

For the well-mixed chemical systems (even divided into nested compartments) often found in cellular biology, interaction and distribution analysis are sufficient to study the system's behaviour. However, there are many other situations, like in cell growth and developmental biology where dynamic spatial arrangements of cells determines fundamental functionalities, where a spatial analysis becomes essential. Thus, a realistic modelling of many cellular phenomena requires space to be taken into account [28].

There are several cases in which the spatial properties of a system could be analysed by just focusing on a finite (and quite limited) number of sectors. If we focus ourselves in this kind of situations, CWC appears to be expressive enough for quite effective descriptions. Indeed, the considerations presented in this paper about the topological organisation of the paradigmatic examples shown in Section 3, also hold for other calculi which are able to express compartmentalisation (see, e.g., BioAmbients [42], Brane Calculi [14], Beta-Binders [21], etc.).

Von Neumann' Cellular Automata [37] were developed as a computational tool inspired by biological behaviour and later used to model biological systems. Cellular Automata are defined by a finite grid of cells, with the state of each cell, evolving in discrete time, affected locally by just the state of the nearby cells. We can mimic the framework of Cellular Automata within CWC by defining a grid in a way similar to what we have done in Section 3.1.

There are other situations, however, where a geometrical distance becomes necessary beyond a purely topological organization (for example in a more detailed analysis in the field of developmental biology).

As a consequence, the need of an extended spatial analysis in systems biology has brought to the extension with (even continuous) spatial features of many formalisms developed for the analysis of biological systems: see, e.g., geometric process algebra [15], spatial P-systems [9], spatial CLS [8] and Bioshape [13].

Theoretically, building a more complex structure over the approach presented in this paper, we could define a geometric space, with coordinates and distance metrics. We might define, e.g., on the lines of the approach presented in [34], a surface language modelling a 2D grid or a 3D space over the CWC model. While adding too many features to the model (e.g., coordinates, position, extension, motion direction and speed, rotation, collision and overlap detection, communication range, etc.) could rise heavily the complexity of this kind of approach, a detailed study on a subset of these features could still be carried out on several systems. We plan to investigate this line of development in near future work.

References

- [1] K. Akiyama, K. Matsuzaki & H. Hayashi (2005): *Plant sesquiterpenes induce hyphal branching in arbuscular mycorrhizal fungi*. *Nature* 435(7043), pp. 824–827, doi:10.1038/nature03608.
- [2] M. Aldinucci, M. Coppo, F. Damiani, M. Drocco, E. Giovannetti, E. Grassi, E. Sciacca, S. Spinella & A. Troina (2010): *CWC Simulator*. Dipartimento di Informatica, Università di Torino. Available at <http://sourceforge.net/projects/cwcsimulator/>.
- [3] M. Aldinucci, M. Coppo, F. Damiani, M. Drocco, M. Torquati & A. Troina (2011): *On Designing Multicore-Aware Simulators for Biological Systems*. In: *Proc. of Intl. Euromicro PDP 2011: Parallel Distributed and network-based Processing*, IEEE Computer Society, pp. 318–325.
- [4] Marco Aldinucci & Massimo Torquati (2009): *FastFlow website*. FastFlow. <http://mc-fastflow.sourceforge.net/>.

- [5] S. Asimi, V. Gianinazzi-Pearson & S. Gianinazzi (1980): *Influence of increasing soil phosphorus levels on interactions between vesicular-arbuscular mycorrhizae and Rhizobium in soybeans*. *Canadian Journal of Botany* 58(20), pp. 2200–2205, doi:10.1139/b80-253.
- [6] R. Barbuti, A. Maggiolo-Schettini, P. Milazzo, P. Tiberi & A. Troina (2008): *Stochastic Calculus of Looping Sequences for the Modelling and Simulation of Cellular Pathways*. *Transactions on Computational Systems Biology* IX, pp. 86–113.
- [7] R. Barbuti, A. Maggiolo-Schettini, P. Milazzo & A. Troina (2006): *A Calculus of Looping Sequences for Modelling Microbiological Systems*. *Fundam. Inform.* 72(1-3), pp. 21–35.
- [8] Roberto Barbuti, Andrea Maggiolo-Schettini, Paolo Milazzo & Giovanni Pardini (2009): *Spatial Calculus of Looping Sequences*. *Electr. Notes Theor. Comput. Sci.* 229(1), pp. 21–39, doi:10.1016/j.entcs.2009.02.003.
- [9] Roberto Barbuti, Andrea Maggiolo-Schettini, Paolo Milazzo, Giovanni Pardini & Luca Tesei (2011): *Spatial P systems*. *Natural Computing* 10(1), pp. 3–16, doi:10.1007/s11047-010-9187-z.
- [10] A. Besserer, V. Puech-Pagès, P. Kiefer, V. Gomez-Roldan, A. Jauneau, S. Roy, J.C. Portais, C. Roux, G. Bécard & N. Séjalon-Delmas (2006): *Strigolactones stimulate arbuscular mycorrhizal fungi by activating mitochondria*. *PLoS Biology* 4(7), pp. 1239–1247, doi:10.1371/journal.pbio.0040226.
- [11] *BioBITs website*. <http://www.biobits.di.unipmn.it/>.
- [12] P. Bonfante-Fasolo (1984): *Anatomy and morphology of VA mycorrhizae*. *VA mycorrhiza*.
- [13] Federico Buti, Diletta Cacciagrano, Flavio Corradini, Emanuela Merelli & Luca Tesei (2010): *BioShape: a spatial shape-based scale-independent simulation environment for biological systems*. *Procedia CS* 1(1), pp. 827–835, doi:10.1016/j.procs.2010.04.090.
- [14] L. Cardelli (2004): *Brane Calculi*. In: *Proc. of CMSB'04, LNCS 3082*, Springer, pp. 257–278.
- [15] Luca Cardelli & Philippa Gardner (2010): *Processes in Space*. In: *Proc. of the 6th international conference on Computability in Europe, CiE'10*, Springer-Verlag, pp. 78–87.
- [16] M. Chabaud, A. Genre, B.J. Sieberer, A. Faccio, J. Fournier, M. Novero, D.G. Barker & P. Bonfante (2011): *Arbuscular mycorrhizal hyphopodia and germinated spore exudates trigger Ca²⁺ spiking in the legume and nonlegume root epidermis*. *New Phytologist* doi:10.1111/j.1469-8137.2010.03464.x.
- [17] M. Coppo, F. Damiani, M. Drocco, E. Grassi, M. Guether & A. Troina (2011): *Modelling Ammonium Transporters in Arbuscular Mycorrhiza Symbiosis*. *Transactions on Computational Systems Biology* XIII, pp. 85–109.
- [18] Mario Coppo, Ferruccio Damiani, Maurizio Drocco, Elena Grassi, Eva Sciacca, Salvatore Spinella & Angelo Troina (2010): *Hybrid Calculus of Wrapped Compartments*. In: *4th International Meeting on Membrane Computing and Biologically Inspired Process Calculi (MeCBIC'10)*, 40, EPTCS, pp. 102–120, doi:10.4204/EPTCS.40.8.
- [19] Mario Coppo, Ferruccio Damiani, Maurizio Drocco, Elena Grassi & Angelo Troina (2010): *Stochastic Calculus of Wrapped Compartments*. In: *8th Workshop on Quantitative Aspects of Programming Languages (QAPL'10)*, 28, EPTCS, pp. 82–98, doi:10.4204/EPTCS.28.6.
- [20] V. Danos & C. Laneve (2004): *Formal molecular biology*. *Theor. Comput. Sci.* 325(1), pp. 69–110, doi:10.1016/j.tcs.2004.03.065.
- [21] P. Degano, D. Prandi, C. Priami & P. Quaglia (2006): *Beta-binders for Biological Quantitative Experiments*. *Electr. Notes Theor. Comput. Sci.* 164(3), pp. 101–117, doi:10.1016/j.entcs.2006.07.014.
- [22] A. Genre & P. Bonfante (2007): *Check-in procedures for plant cell entry by biotrophic microbes*. *Molecular Plant-Microbe Interactions* 20(9), pp. 1023–1030, doi:10.1094/MPMI-20-9-1023.
- [23] A. Genre, M. Chabaud, T. Timmers, P. Bonfante & D.G. Barker (2005): *Arbuscular mycorrhizal fungi elicit a novel intracellular apparatus in Medicago truncatula root epidermal cells before infection*. *The Plant Cell Online* 17(12), p. 3489, doi:10.1105/tpc.105.035410.
- [24] D. Gillespie (1977): *Exact stochastic simulation of coupled chemical reactions*. *J. Phys. Chem.* 81, pp. 2340–2361, doi:10.1021/j100540a008.

- [25] M.J. Harrison (2005): *Signaling in the arbuscular mycorrhizal symbiosis*. *Annu. Rev. Microbiol.* 59, pp. 19–42, doi:10.1146/annurev.micro.58.030603.123749.
- [26] C.M. Hepper (1983): *The effect of nitrate and phosphate on the vesicular-arbuscular mycorrhizal infection of lettuce*. *New Phytologist* 93(3), pp. 389–399, doi:10.1111/j.1469-8137.1983.tb03439.x.
- [27] H. Javot, R.V. Penmetsa, N. Terzaghi, D.R. Cook & M.J. Harrison (2007): *A Medicago truncatula phosphate transporter indispensable for the arbuscular mycorrhizal symbiosis*. *Proceedings of the National Academy of Sciences* 104(5), p. 1720, doi:10.1073/pnas.0608136104.
- [28] B. Kholodenko (2006): *Cell-signalling dynamics in time and space*. *Nature Reviews Molecular Cell Biology* 7, pp. 165–176, doi:10.1038/nrm1838.
- [29] S. Kosuta, M. Chabaud, G. Loughon, C. Gough, J. Dénarié, D.G. Barker & G. Bécard (2003): *A Diffusible Factor from Arbuscular Mycorrhizal Fungi Induces Symbiosis-Specific MtENOD11 Expression in Roots of Medicago truncatula*. *Plant Physiology* 131(3), p. 952, doi:10.1104/pp.011882.
- [30] S. Kosuta, S. Hazledine, J. Sun, H. Miwa, R.J. Morris, J.A. Downie & G.E.D. Oldroyd (2008): *Differential and chaotic calcium signatures in the symbiosis signaling pathway of legumes*. *Proceedings of the National Academy of Sciences* 105(28), p. 9823, doi:10.1073/pnas.0803499105.
- [31] J. Krivine, R. Milner & A. Troina (2008): *Stochastic Bigraphs*. *Electron. Notes Theor. Comput. Sci.* 218, pp. 73–96, doi:10.1016/j.entcs.2008.10.006.
- [32] J.A. López-Ráez, T. Charnikhova, V. Gómez-Roldán, R. Matusova, W. Kohlen, R. De Vos, F. Verstappen, V. Puech-Pages, G. Bécard, P. Mulder et al. (2008): *Tomato strigolactones are derived from carotenoids and their biosynthesis is promoted by phosphate starvation*. *New Phytologist* 178(4), pp. 863–874, doi:10.1111/j.1469-8137.2008.02406.x.
- [33] R. Matusova, K. Rani, F.W.A. Verstappen, M.C.R. Franssen, M.H. Beale & H.J. Bouwmeester (2005): *The strigolactone germination stimulants of the plant-parasitic Striga and Orobanche spp. are derived from the carotenoid pathway*. *Plant Physiology* 139(2), p. 920, doi:10.1104/pp.105.061382.
- [34] Sara Montagna & Mirko Viroli (2010): *A Framework for Modelling and Simulating Networks of Cells*. *Electr. Notes Theor. Comput. Sci.* 268, pp. 115–129, doi:10.1016/j.entcs.2010.12.009.
- [35] B. Mosse (1973): *Advances in the study of vesicular-arbuscular mycorrhiza*. *Annual Review of Phytopathology* 11(1), pp. 171–196, doi:10.1146/annurev.py.11.090173.001131.
- [36] G. Nagahashi & D.D. Douds Jr (2000): *Partial separation of root exudate components and their effects upon the growth of germinated spores of AM fungi*. *Mycological Research* 104(12), pp. 1453–1464, doi:10.1017/S0953756200002860.
- [37] John Von Neumann (1966): *Theory of Self-Reproducing Automata*. University of Illinois Press, Champaign, IL, USA.
- [38] G.E.D. Oldroyd & J.A. Downie (2008): *Coordinating nodule morphogenesis with rhizobial infection in legumes*. *Annu. Rev. Plant Biol.* 59, pp. 519–546, doi:10.1146/annurev.arplant.59.032607.092839.
- [39] Nicolas Oury & Gordon Plotkin (2011): *Multi-Level Modelling via Stochastic Multi-Level Multiset Rewriting*. Draft submitted to MSCS.
- [40] C. Priami, A. Regev, E. Y. Shapiro & W. Silverman (2001): *Application of a stochastic name-passing calculus to representation and simulation of molecular processes*. *Inf. Process. Lett.* 80(1), pp. 25–31, doi:10.1016/S0020-0190(01)00214-9.
- [41] G. Păun (2002): *Membrane computing. An introduction*. Springer.
- [42] A. Regev, E. M. Panina, W. Silverman, L. Cardelli & E. Y. Shapiro (2004): *BioAmbients: an abstraction for biological compartments*. *Theor. Comput. Sci.* 325(1), pp. 141–167, doi:10.1016/j.tcs.2004.03.061.
- [43] A. Regev & E. Shapiro (2002): *Cells as computation*. *Nature* 419, p. 343, doi:10.1007/3-540-36481-1_1.
- [44] C. Sbrana & M. Giovannetti (2005): *Chemotropism in the arbuscular mycorrhizal fungus Glomus mosseae*. *Mycorrhiza* 15(7), pp. 539–545, doi:10.1007/s00572-005-0362-5.

- [45] E Sciacca, S Spinella, A Genre & C Calcagno (2011): *Analysis of Calcium Spiking in Plant Root Epidermis through CWC Modeling*. In: *CS2BIO11*, pp. 1–12.
- [46] R. Toth & R.M. Miller (1984): *Dynamics of arbuscule development and degeneration in a Zea mays mycorrhiza*. *American journal of botany* 71(4), pp. 449–460, doi:10.2307/2443320.
- [47] K. Yoneyama, Y. Takeuchi & T. Yokota (2001): *Production of clover broomrape seed germination stimulants by red clover root requires nitrate but is inhibited by phosphate and ammonium*. *Physiologia Plantarum* 112(1), pp. 25–30, doi:10.1034/j.1399-3054.2001.1120104.x.

Appendix A: Quorum Sensing and Molecular Diffusion Model

Pseudomonas aeruginosa uses quorum sensing to keep low the expression of virulence factors until the colony has reached a certain density, when an autoinduced production of virulence factors is started. The bacterium membrane, denoted as m , contains only a DNA strand. The DNA is modelled as a sequence of genes $lasO$ $lasR$ $lasI$ (atom $LasORI$), where $lasO$ represents the target to which a complex autoinducer/R-protein binds to promote transcription. The following rewrite rules model the system behaviour (the kinetics are taken from [6]):

$$\begin{array}{ll}
 (R_1) \quad m : LasORI \xrightarrow{20} LasORI LasR & (R_2) \quad m : LasORI \xrightarrow{5} LasORI LasI \\
 (R_3) \quad m : LasI \xrightarrow{8} LasI oxo3 & (R_4) \quad m : oxo3 LasR \xrightarrow{0.25} R3 \\
 (R_5) \quad m : R3 \xrightarrow{400} oxo3 LasR & (R_6) \quad m : R3 LasORI \xrightarrow{0.25} RO3 \\
 (R_7) \quad m : RO3 \xrightarrow{10} R3 LasORI & (R_8) \quad m : RO3 \xrightarrow{1200} RO3 LasR \\
 (R_9) \quad m : RO3 \xrightarrow{300} RO3 LasI & (R_{10}) \quad m : LasI \xrightarrow{1} \bullet \\
 (R_{11}) \quad m : LasR \xrightarrow{1} \bullet & (R_{12}) \quad m : oxo3 \xrightarrow{1} \bullet \\
 (R_{13}) \quad m : I oxo3 \xrightarrow{0.1} A oxo3 &
 \end{array} \tag{8}$$

Rules R_1 and R_2 describe the production from the DNA of proteins $LasR$ and $LasI$, respectively. Rule R_3 describes the production of the autoinducer, modelled as atom $oxo3$, performed by the $LasI$ enzyme. Rules R_4 and R_5 describe the complexation and decomplexation of the autoinducer and the $LasR$ protein, where the complex is denoted $R3$. Rules R_7 , R_8 , R_9 describe the binding of the activated autoinducer (the $RO3$ complex) to the DNA and its influence in the production of $LasR$ and $LasI$. Finally, rules R_{10} , R_{11} , R_{12} describe the degradation of proteins. In particular, rule R_{12} models the degradation of the autoinducer, which can happen both inside and outside the bacterium. Bacteria are marked as “active” (atom A) when reaching a sufficient high level of auto-inducer inside the respective sector otherwise they are marked as “inactive” (atom I).

The following rules describe the ability of the autoinducer to cross the membrane, in both directions inside the sectors (different kinetics are used to model the different bandwidths of the channels). An autoinducer inside the bacterium is modelled as a non-positional element, while autoinducers outside have an associated spatial sector S_i for $i = 1, \dots, 4$:

$$\begin{array}{ll}
 S_i : (x \mid oxo3 X)^m \xrightarrow{30} oxo3(x \mid X)^m & \\
 S_i : oxo3(x \mid X)^m \xrightarrow{1} (x \mid oxo3 X)^m & \\
 S_i : oxo3 \xrightarrow{1} \bullet &
 \end{array} \tag{9}$$

$i \backslash j$	1	2	3	4
1	ND	0.0	0.0	0.1
2	0.0	ND	0.2	0.3
3	0.0	0.2	ND	0.3
4	0.1	0.3	0.3	ND

Table 1: Values for the kinetic rates k_{ij}

The diffusion of the autoinducer across the different sectors is described by the following rules:

$$\top : (x \rfloor \text{oxo3 } X)^{S_i} (y \rfloor Y)^{S_j} \xrightarrow{k_{ij}} (x \rfloor X)^{S_i} (y \rfloor \text{oxo3 } Y)^{S_j} \quad (10)$$

where k_{ij} is related to the sectors channel capacities. In our experiments the values of k_{ij} are shown in Table 1 where $k_{ij} = k_{ji}$.

The simulations were carried out using the following initial term T (see Figure 2):

$$\begin{aligned} T_1 &= (\rfloor 10 * (\rfloor I \text{ LasORI})^m)^{S_1} & T_2 &= (\rfloor 15 * (\rfloor I \text{ LasORI})^m)^{S_2} \\ T_3 &= (\rfloor 15 * (\rfloor I \text{ LasORI})^m)^{S_3} & T_4 &= (\rfloor 8 * (\rfloor I \text{ LasORI})^m)^{S_4} \\ T &= T_1 T_2 T_3 T_4 \end{aligned} \quad (11)$$

The model above can be easily enriched by adding rules describing also the movement of the bacteria between the different sectors and bacteria replication.